

RESEARCH ARTICLE

A Spectroscopic Approach to Investigate the Molecular Interactions between the Newly Approved Irreversible ErbB blocker "Afatinib" and Bovine Serum Albumin

Amer M. Alanazi[☉], Ali Saber Abdelhameed^{*☉}

Department of Pharmaceutical Chemistry, College of Pharmacy, King Saud University, P.O. Box 2457, Riyadh, 11451, Saudi Arabia

☉ These authors contributed equally to this work.

* asaber@ksu.edu.sa



OPEN ACCESS

Citation: Alanazi AM, Abdelhameed AS (2016) A Spectroscopic Approach to Investigate the Molecular Interactions between the Newly Approved Irreversible ErbB blocker "Afatinib" and Bovine Serum Albumin. PLoS ONE 11(1): e0146297. doi:10.1371/journal.pone.0146297

Editor: Jamshidkhan Chamani, Islamic Azad University-Mashhad Branch, Mashhad, Iran, ISLAMIC REPUBLIC OF IRAN

Received: October 13, 2015

Accepted: December 15, 2015

Published: January 11, 2016

Copyright: © 2016 Alanazi, Abdelhameed. This is an open access article distributed under the terms of the [Creative Commons Attribution License](https://creativecommons.org/licenses/by/4.0/), which permits unrestricted use, distribution, and reproduction in any medium, provided the original author and source are credited.

Data Availability Statement: All relevant data are within the paper and its Supporting Information file.

Funding: This study was funded by the Deanship of Scientific Research at King Saud University through research group No. RG-1435-025. The funders had no role in study design, data collection and analysis, decision to publish, or preparation of the manuscript.

Competing Interests: The authors have declared that no competing interests exist.

Abstract

The interaction of afatinib (AFB) with bovine serum albumin (BSA) was examined *via* fluorescence and UV-Vis spectroscopy. Spectrofluorimetric measurements revealed that AFB can strongly quench the BSA intrinsic fluorescence through producing a non-fluorescent complex. This quenching mechanism was thoroughly investigated with regard to the type of quenching, binding constant, number of binding locations and the fundamental thermodynamic parameters. Subsequently, the association constant of AFB with BSA was computed at three different temperatures and was found to range from 7.34 to 13.19 $\times 10^5$ L mol⁻¹. Thermodynamic parameters calculations demonstrated a positive ΔS^\ominus value with both negative ΔH^\ominus and ΔG^\ominus values for AFB–BSA complex, which in turn infers that a spontaneous binding is taking place with both electrostatic bonding and hydrophobic interactions participating in the binding of AFB and BSA. Similarly, the UV absorption spectra of AFB-BSA system were studied and confirmed the interaction. Conformational alteration of the protein upon binding to AFB was elaborated with the aid of three dimensional fluorescence measurements as well as synchronous fluorescence spectra.

Introduction

Afatinib (AFB; formerly known as BIBW 2992) ([Fig 1](#)), is an orally administered selective irreversible ErbB family blocker (EGFR/ErbB1, HER2/ErbB2 and ErbB4) with has wide-spectrum pre-clinical efficacy against EGFR mutations [1]. Due to the fact that, these receptors are essential in cellular proliferation and apoptosis, their inhibition by AFB may prevent tumor growth and spread. AFB is now marketed as Gilotrif[®] tablets (Boehringer-Ingelheim pharmaceuticals, Inc. USA) in the form of afatinib di-maleate salt equivalent to 20, 30, and 40 mg afatinib base. AFB was granted the FDA approval for the management of patients with metastatic or locally advanced non-small cell lung cancer (NSCLC) with their tumors possess epidermal growth

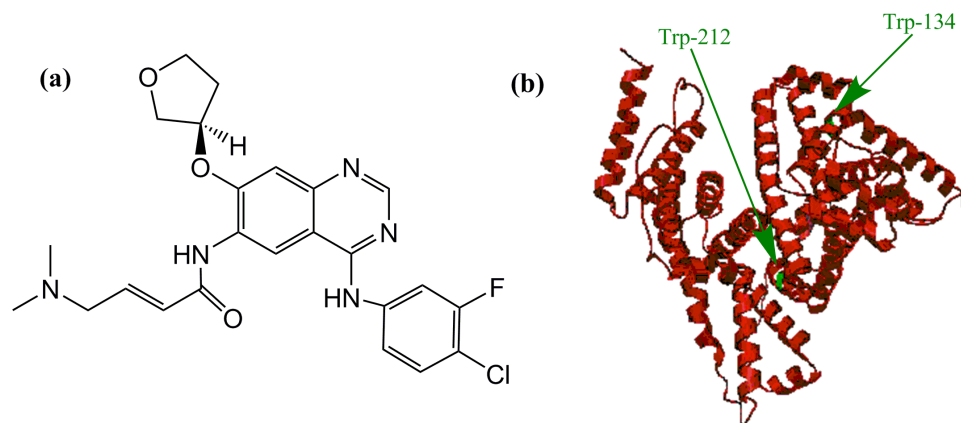


Fig 1. Chemical structure of AFB (a) and ribbon representation of BSA (b).

doi:10.1371/journal.pone.0146297.g001

factor receptor (EGFR) exon 21 (L858R) substitution mutations or exon 19 deletions [2]. Therefore and with the advancement of drug development in cancer management, various possible interactions should be taken into account. Concomitantly, serum albumins, the multifunctional depots and transport carriers, are considered the predominant circulatory proteins in various organisms (50–60% of the total amount of plasma proteins) [3]. Serum albumins have been extensively studied in terms of their structural and physiological properties [4–6]. Their interaction with the different drugs may strongly influence the drugs' apparent distribution volume as well as elimination rate. Therefore, studies on the drug-protein binding will aid in the interpretation of the metabolism and transport mechanism of the drug. An interesting member of the albumins family, is the bovine serum albumin (BSA) which also possess various physiological properties that involve its binding, conveying and delivery of a wide range of molecules [5,7–9]. Serum albumins are responsible for certain conformational dynamics and binding aggregation in solution [10]. BSA is structurally homologue to its human counterpart (HSA) with a well-studied structure [11–15]. Hence, the binding of the various drugs to BSA and serum albumins, in general, is an essential factor to determine the drug's possible pharmacokinetic and pharmacodynamics profile. Several earlier investigations have reported the BSA-drugs interaction using spectroscopic tools [10,16–18] including recent studies of other members of the tyrosine kinase family [19,20]. In the present study, the intrinsic fluorescence of BSA quenched by AFB was investigated by the selective excitation of BSA's tryptophan residues present at positions 134 and 212 of the 583 amino acids polypeptide chain [21–23] (Fig 1b). Thorough literature survey revealed that no single study was reported for investigating AFB and serum albumin binding. Therefore, the current work is sought to investigate the interaction of BSA and AFB utilizing fluorescence spectroscopy to provide an insight into their molecular interaction.

Materials and Methods

Materials

Unless otherwise stated all chemicals, reagents and solvents were of analytical grade and procured from BDH laboratory supplies (Poole, UK). Afatinib reference standard was acquired from Weihua Pharma Co. Ltd (Zhejiang, China). Techno Pharmchem (Haryana, India) supplied the bovine serum albumin (BSA). Ultrapure water of 18.2 M Ω was produced from a Millipore Milli-Q[®] UF-Plus purification system (Millipore, MA, USA).

Instruments and conditions

Fluorescence measurements were carried out in a 1-cm quartz cell with slits of 5nm (for excitation and emission) and $\lambda_{ex} = 280$ and monitoring at $\lambda_{em} = 338$ using a Jasco FP-8200 (Jasco International Co. Ltd. Tokyo, Japan). The AFB quenching effect on BSA was investigated at its maximum emission range (334–344 nm). All UV-Vis absorbance spectral determinations were performed on a Nanodrop™ 2000 UV-Vis spectrophotometer (Thermo Scientific, Wilmington, DE, USA). Experimental solutions were all made in 1X phosphate buffered saline (PBS buffer) pH 7.4, with the pH recorded using an Adwa AD1030 pH-meter (ADWA Instruments Inc., Romania).

Sample preparation

All solutions were prepared at room temperature, and were kept at -20°C . AFB was dissolved in methanol preparing a stock solution of 1.0 mgmL^{-1} . Further, AFB solution was diluted (1.0 mL of stock solution) by 10 ml with methanol to yield a $100 \text{ }\mu\text{gmL}^{-1}$ solution. Subsequent dilution of the latter solution was carried out using PBS buffer pH 7.4 producing a working solution of $20 \text{ }\mu\text{gmL}^{-1}$.

A 1.0 mgmL^{-1} solution of bovine serum albumin (BSA) was prepared in PBS buffer pH 7.4 and kept in a cool, dark place. Subsequent dilutions of BSA stock solution were made in PBS buffer pH 7.4 yielding a $100 \text{ }\mu\text{gmL}^{-1}$ working solution.

Protein Concentration determination

Protein concentration was determined from the specific extinction coefficient of $A^{1\%}_{280} \sim 6.7$ for BSA using Nanodrop™ 2000 UV-Vis spectrophotometer (Thermo Scientific, Wilmington, DE, USA). Prior to measurements, BSA samples were filtered through $0.45 \text{ }\mu\text{m}$ syringe filters.

AFB–protein interactions

Following several preliminary spectrofluorimetric measurements of AFB and BSA, an optimum concentration of $100 \text{ }\mu\text{gmL}^{-1}$ was chosen for BSA with the drug concentration varying in the range of $0.3\text{--}10 \text{ }\mu\text{gmL}^{-1}$. Fluorescence spectra were recorded at three different temperatures of 288, 298 and 309 K over a scan range of $\lambda_{em} 290\text{--}500 \text{ nm}$ after being excited at $\lambda_{ex} 280 \text{ nm}$. To reduce the inner filter effect, both intensities of the fluorescence arising from excitation light absorption and emission light re-absorption were corrected using [eq \(1\)](#) [24,25]

$$F_{cor} = F_{obs} \times e^{(A_{ex} + A_{em})/2} \quad (1)$$

Here, the corrected and observed fluorescence intensities are represented as F_{cor} and F_{obs} , respectively. While, values of the AFB absorbance at excitation and emission wavelengths are represented as A_{ex} and A_{em} , respectively.

UV-Vis spectrophotometric determinations

UV-Vis absorption determinations of BSA in the presence and absence of AFB were made in the range of 220–350 nm. BSA concentration was kept constant at 1.0 mgmL^{-1} with using AFB concentration of 5.0 and $10.0 \text{ }\mu\text{gmL}^{-1}$ for binding measurements and $1.0 \text{ }\mu\text{gmL}^{-1}$ for AFB reference measurement.

Results and Discussion

Fluorescence Measurements

Fluorescence measurements among a variety of spectroscopic tools can yield plenty of information of the binding of proteins and/or small molecules to proteins, such as the binding mechanism, type, binding parameters, conformational changes, *etc.* [26–28]. Quenching of the fluorescence indicates reduction of the fluorescence intensity of a given fluorophore *via* different molecular interactions [29,30]. The fluorescence spectra of BSA in absence and presence of a concentration series of different AFB were determined in the range of λ_{em} 290–500 nm following excitation at λ_{ex} 280 nm. AFB resulted in quenching of the BSA fluorescence intensity in a linear manner (Fig 2) without affecting the BSA emission wavelength and shape of the peak. The observed results reflect a complex formation between AFB and BSA [31].

Fluorescence quenching mechanism

Fluorescence quenching mechanisms are categorized into dynamic quenching and static-quenching [12,32]. Dynamic quenching is a result of diffusion whereas static type of quenching is basically due to formation of a ground state complex. Moreover, both types have different temperature dependence *viz.* quenching constants are supposed to increase at higher temperatures in dynamic quenching. Conversely, a diminished stability and lower quenching constants are favored with elevated temperature in static quenching. Quenching results were interpreted using the Stern–Volmer (Eq 2) [33] and Lineweaver–Burk mathematical formulas (Eq 3) [34], both equations have been commonly reported to describe dynamic and static quenching.

$$F_0/F = 1 + K_{SV}C_Q = 1 + K_q\tau_0C_Q \quad (2)$$

$$(F_0 - F)^{-1} = F_0^{-1} + K_{LB}^{-1}F_0^{-1}C_Q^{-1} \quad (3)$$

Where F_0 and F the fluorescence intensities of BSA without and with the addition of AFB, respectively, C_Q the concentration of AFB (quencher) and, K_{SV} , K_{LB} are the Stern–Volmer and Lineweaver–Burk constants, respectively. While, the quenching rate constant is K_q and τ_0 is the mean protein lifetime in absence of the quencher. Previous reports have demonstrated that, over a defined range of concentration, if the quenching type is single static or dynamic quenching then the curve of F_0/F versus C_Q (Stern–Volmer curve) would be linear [16]. Whilst, a linear curve of $(F_0 - F)^{-1}$ versus C_Q^{-1} (Lineweaver–Burk curve) is an indication of a static quenching [35]. On the other hand, an ascending curvature of the Stern–Volmer plot refers to combined (dynamic and static) quenching [36]. It can be observed from Fig 3a that the binding of AFB and BSA result in linear Stern–Volmer curves at lower AFB concentration ($0.3\text{--}3.0 \mu\text{g}\cdot\text{mL}^{-1}$) which become significantly upward bent at higher AFB concentrations ($5.0\text{--}10.0 \mu\text{g}\cdot\text{mL}^{-1}$). This supports the hypothesis of a single quenching (static or dynamic quenching) at lower AFB concentration, while a combined quenching (both static and dynamic) would be more appropriate at higher AFB concentrations. Additionally, Fig 3b of the Lineweaver–Burk plots ($0.3\text{--}10.0 \mu\text{g}\cdot\text{mL}^{-1}$) demonstrate that under the studied concentration range of AFB, the curves of $(F_0 - F)^{-1}$ vs. C_Q^{-1} were linear that infers the presence of clear characteristics of a static quenching. Furthermore, the K_{SV} and K_{LB} values summarized in Table 1 are decreasing upon the steady increase in temperature that in turn is in a good agreement with the static quenching hypothesis [36].

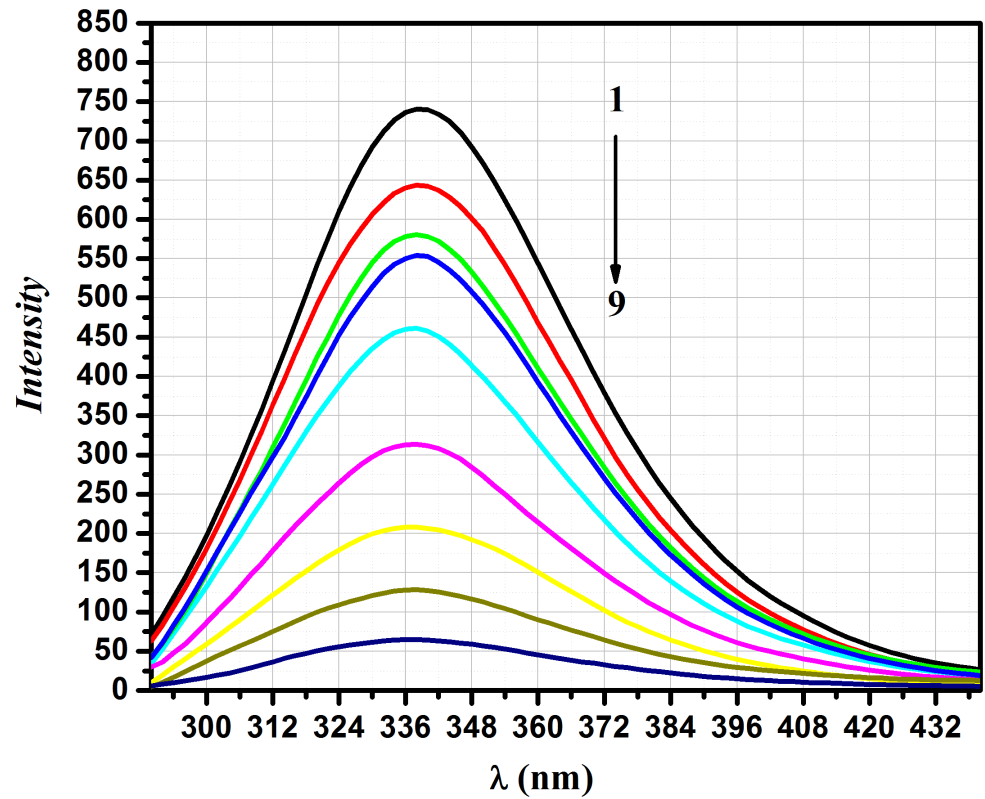


Fig 2. Emission spectra of BSA ($100 \mu\text{g.mL}^{-1}$) only (1) and following BSA binding to AFB at a concentration series of $0.3 \mu\text{g.mL}^{-1}$ (2), $0.4 \mu\text{g.mL}^{-1}$ (3), $0.5 \mu\text{g.mL}^{-1}$ (4), $1.0 \mu\text{g.mL}^{-1}$ (5), $3.0 \mu\text{g.mL}^{-1}$ (6), $5 \mu\text{g.mL}^{-1}$ (7), $7.0 \mu\text{g.mL}^{-1}$ (8) and $10 \mu\text{g.mL}^{-1}$ (9).

doi:10.1371/journal.pone.0146297.g002

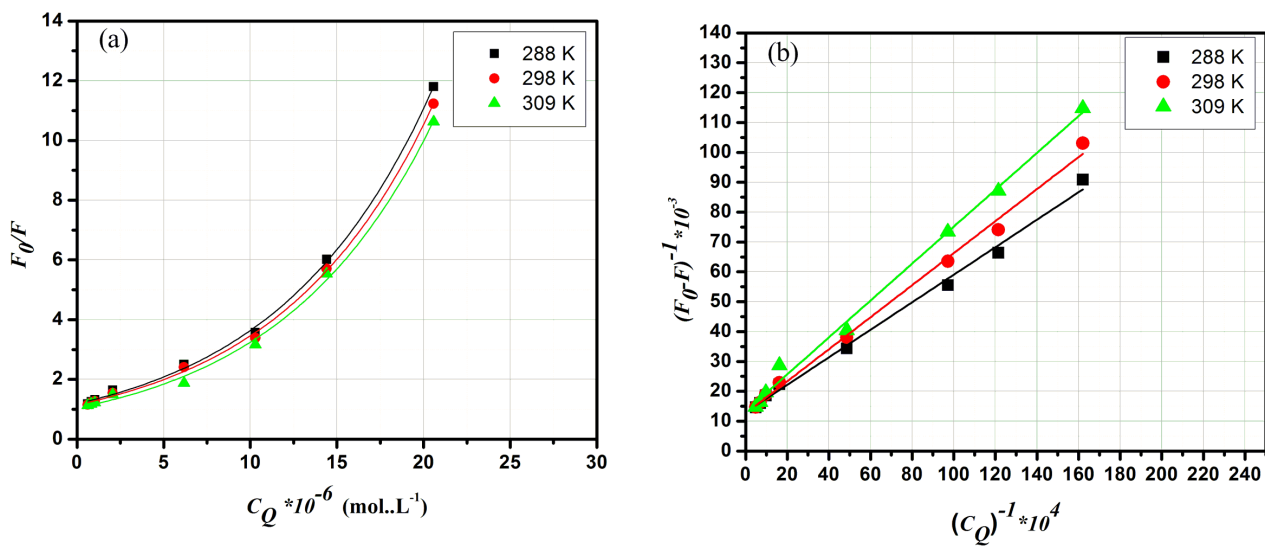


Fig 3. Stern–Volmer (a) and Lineweaver–Burk (b) plots at various temperatures.

doi:10.1371/journal.pone.0146297.g003

Table 1. Parameters computed from both Stern-Volmer and Lineweaver–Burk relations for AFB-BSA binding.

Temperature (T)/K	Stern-Volmer parameters			Lineweaver–Burk parameters	
	$K_{SV} \times 10^5 (\text{Lmol}^{-1})$	$K_q \times 10^{13} (\text{Lmol}^{-1}\text{s}^{-1})$	r^2	$K_{LB} \times 10^5 (\text{Lmol}^{-1})$	r^2
288	1.12±0.087	1.12	0.9986	2.82±0.12	0.9948
298	1.09±0.084	1.09	0.9987	2.35±0.11	0.9956
309	1.04±0.134	1.04	0.9970	2.15±0.12	0.9955

doi:10.1371/journal.pone.0146297.t001

Moreover, the formation of a non-fluorescent complex was confirmed by the quenching rate constants, K_q , values shown in Table 1, which were calculated using eq 4

$$K_q = K_{SV} / \tau_0 \tag{4}$$

Where the value of τ_0 (average protein lifetime without the quencher), τ_0 of a biopolymer is 10^{-8}s^{-1} [37]. The obtained K_q values are higher than the previously reported values for various quenchers with the biopolymer of $2 \times 10^{10} \text{LM}^{-1}\text{s}^{-1}$ [37]. This in turn infers that the quenching in case of AFB-BSA is a result of a complex formation and not induced by dynamic collision [35].

Binding mode and binding sites

Presuming independent binding of small molecules to a group of equivalent sites on a macromolecule, hence, eq 5 can explain the equilibrium between free and bound molecules [36,38]:

$$\log\left(\frac{F_0 - F}{F}\right) = \log K + n \log C_Q \tag{5}$$

In this equation (Eq 5) the binding constant is referred to as K while, binding sites number on a BSA molecule is n . Plotting $\log(F_0 - F)/F$ vs. $\log C_Q$ (S1 Fig) could yield K and n values which are summarized in Table 2 at the investigated temperatures. These values demonstrate a reduction in the binding constant and to a lesser extent the n value with the increase in temperature, producing a less stable afatinib–BSA complex. Furthermore, n values were found to be nearly ~1 that infers the existence of one association site between BSA and afatinib.

Thermodynamics parameters and nature of the binding forces

Thermodynamic variants namely, enthalpy (ΔH^\ominus) and entropy (ΔS^\ominus) of AFB–BSA interaction are significant to confirm the binding forces. The thermodynamic process is deemed responsible for formation of the complex as the binding constant depends on primarily on temperature. In general, the interaction of a ligand and a macromolecule may involve one or more of the different binding forces viz van der Waals, hydrophobic, electrostatic forces and/or formation of hydrogen bonds. Previous reports including our group’s findings on the sign and magnitude of

Table 2. Summary of the thermodynamic parameters for AFB-BSA interaction along with binding parameters K and n .

Temperature(T) (K)	$\Delta G^\ominus (\text{kJmol}^{-1})$	$\Delta H^\ominus (\text{kJmol}^{-1})$	$\Delta S^\ominus (\text{Jmol}^{-1}\text{K}^{-1})$	$K \times 10^5 (\text{Lmol}^{-1})$	n^*	r^2
288	-33.75±0.04	-20.69±0.62	45.34±2.85	13.19±0.14	1.13±0.01	0.9787
298	-34.19±0.07			9.87±0.46	1.09±0.01	0.9771
309	-34.69±0.12			7.34±0.31	1.07±0.01	0.9745

* All values are average of three determinations

doi:10.1371/journal.pone.0146297.t002

the different thermodynamic parameter associated with the various types of protein-ligand interactions [39–44] concluded that, a hydrophobic interaction is consistent with positive ΔH^θ and ΔS^θ of a system, while hydrogen bonding and van der Waals forces result in negative ΔH^θ and ΔS^θ values. Additionally, involvement of the electrostatic forces usually renders a negative ΔH^θ and a positive ΔS^θ [39–44]. In the present study, thermodynamic parameters of the AFB-BSA system were computed using eqs 6 and 7:

$$\ln K = \frac{-\Delta H^\theta}{RT} + \frac{\Delta S^\theta}{R} \quad (6)$$

$$\Delta G^\theta = \Delta H^\theta - T \cdot \Delta S^\theta \quad (7)$$

In these equations, binding constant is referred to with the letter K while R stands for the gas constant, while T is temperature (in Kelvins) and ΔG^θ is the free energy change. Hence, plotting the values of $\ln K$ on the y -axis and $1/T$ on the x -axis (Fig 4) will result in the calculation of ΔH^θ , ΔG^θ and ΔS^θ .

Based on the previously mentioned rules for the main binding forces, the results summarized in Table 2 reveal that the AFB-BSA binding can not be accounted for as a single intermolecular force model. As from the water structure point of view, a positive ΔS^θ value is usually considered an evidence for hydrophobic interaction [38,44]. Additionally, for AFB-BSA system under our experimental pH of 7.4, AFB is over 96% ionized based on its predicted pKa value (8.81 due to the dimethylamine moiety); along with the obtained negative ΔH^θ and positive ΔS^θ , so electrostatic interaction cannot be excluded from the binding. Hence, it is probably that hydrophobic and electrostatic forces are involved in this binding process

UV–vis absorption spectra

Fig 5 shows the measured absorption spectra for AFB and BSA and proves the formation of a complex between AFB and BSA. Moreover, the UV absorption intensity enhanced gradually

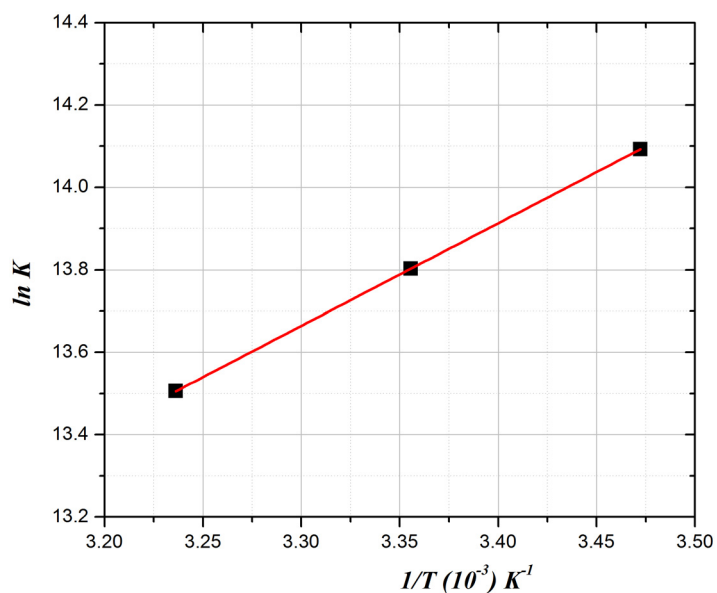


Fig 4. A representative Van't Hoff plot for AFB-BSA binding.

doi:10.1371/journal.pone.0146297.g004

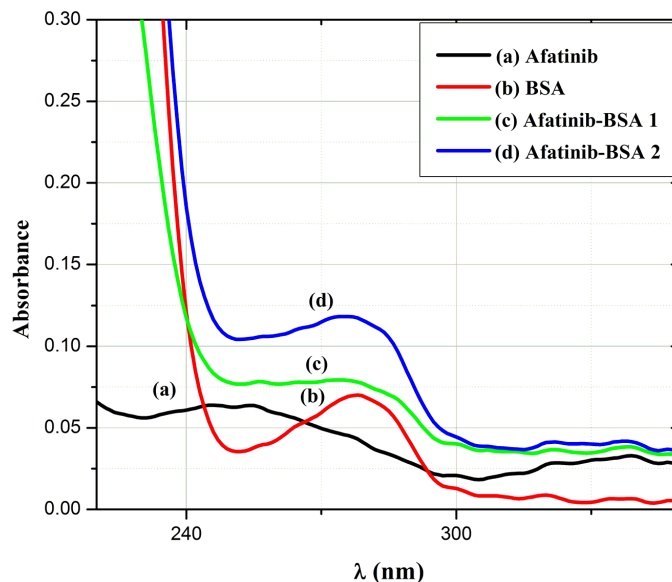


Fig 5. UV spectra of (a) 1.0 $\mu\text{g mL}^{-1}$ AFB (b) 1.0 mg mL^{-1} BSA (c) AFB (5.0 $\mu\text{g mL}^{-1}$)+BSA(1.0 mg mL^{-1}) (d) AFB (10.0 $\mu\text{g mL}^{-1}$)+BSA(1.0 mg mL^{-1}).

doi:10.1371/journal.pone.0146297.g005

for BSA following addition of AFB concentrations, which may infer the extension of the BSA peptide strands with the AFB gradual increment.

Effect of AFB on BSA Conformation

Synchronous fluorescence. Synchronous fluorescence spectra of BSA indicates the fluorescence of tyrosine (Tyr) and tryptophan residues (Trp.) of BSA at wavelength intervals of $\Delta\lambda$ is 15 nm and 60 nm, respectively[45,46]. It can be seen from Fig 6 that the intensity of the emission spectra of Tyr. and Trp. was diminished with no clear peak shift. Comparing the

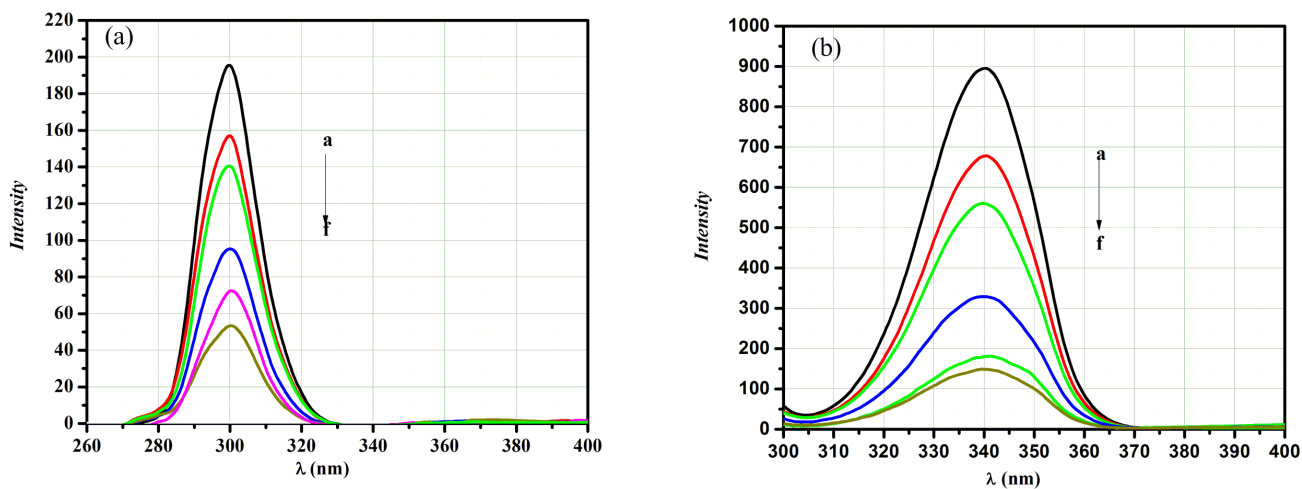


Fig 6. Spectra of the synchronous fluorescence of BSA (100 $\mu\text{g.mL}^{-1}$) with the addition of AFB (a-f) = (0, 0.5, 1.0, 3.0, 5.0 and 10.0 $\mu\text{g.mL}^{-1}$) at (a) $\Delta\lambda = 15 \text{ nm}$ (b) $\Delta\lambda = 60 \text{ nm}$.

doi:10.1371/journal.pone.0146297.g006

Table 3. Parameters of the 3D fluorescence for AFB-BSA binding.

	BSA		AFB-BSA	
	1 st Peak	2 nd Peak	1 st Peak	2 nd Peak
Position of the peak ($\lambda_{ex}/\lambda_{em}$, nm/nm)	224/336	278/334	224/336	278/334
Relative intensity (RFI)	9993.22	4258.31	2845.65	1290.87
Stokes shift $\Delta\lambda$ /nm	112	56	112	52

doi:10.1371/journal.pone.0146297.t003

quenching effect of AFB on the fluorescence intensity of Tyr. and Trp. residues, it is clear that a Trp. Quenching is more significant, which may refer to that the binding site of AFB nearer to tryptophan residues.

Three dimensional fluorescence measurements. Measurements of the three-dimensional (3D) fluorescence were performed with the calculations of different characteristic 3D parameters are reported in Table 3. Figs 7 and 8 show that BSA possess different fluorescence peaks, where, peak 1, ($\lambda_{ex}224 \rightarrow \lambda_{em}336$) which essentially refers to the fluorescence feature of $n \rightarrow \pi^*$ transition of the polypeptide backbone of BSA structure, $C = O$ [47]. While, peak 2, ($\lambda_{ex}278 \rightarrow \lambda_{em}334$) infers the spectral attributes of Trp. and Tyr. residues[18]. With its binding to AFB the BSA fluorescence peaks were quenched as evidenced from Figs 7b and 8b.

Conclusions

The current study provided an approach for investigating the interactions of the new tyrosine kinase inhibitor, afatinib (AFB), with BSA for the first time using fluorescence-quenching technique. AFB was shown to quench the fluorescence of BSA *via* static type of binding and formation of a non-fluorescent complex. Binding constant for AFB-BSA complex was computed to be in the order of 10^5 Lmol^{-1} . The calculated thermodynamic parameters were consistent with the rule of $\Delta G^\theta < 0$; $\Delta H^\theta < 0$; $\Delta S^\theta > 0$ which mainly infer a spontaneous interaction that may involve both hydrophobic and electrostatic binding forces. Since serum albumins are known to have diverse functions, particularly as carrier molecules for several drugs. The work presented in this study can form an important tool in assessing the pharmacological properties of AFB when used in cancer patients.

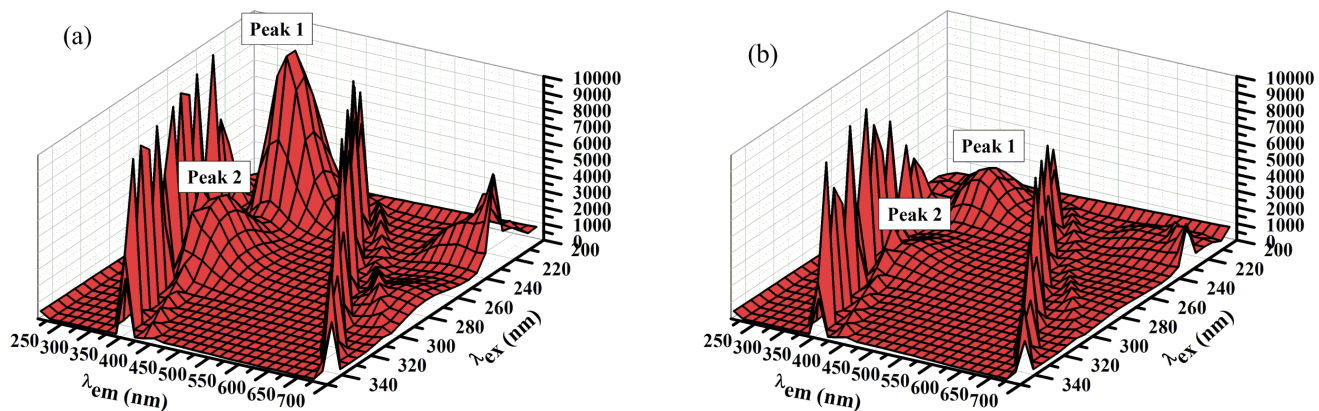


Fig 7. 3D spectra of BSA ($100 \mu\text{g.mL}^{-1}$) in (a) absence and (b) presence of AFB ($5 \mu\text{g.mL}^{-1}$).

doi:10.1371/journal.pone.0146297.g007

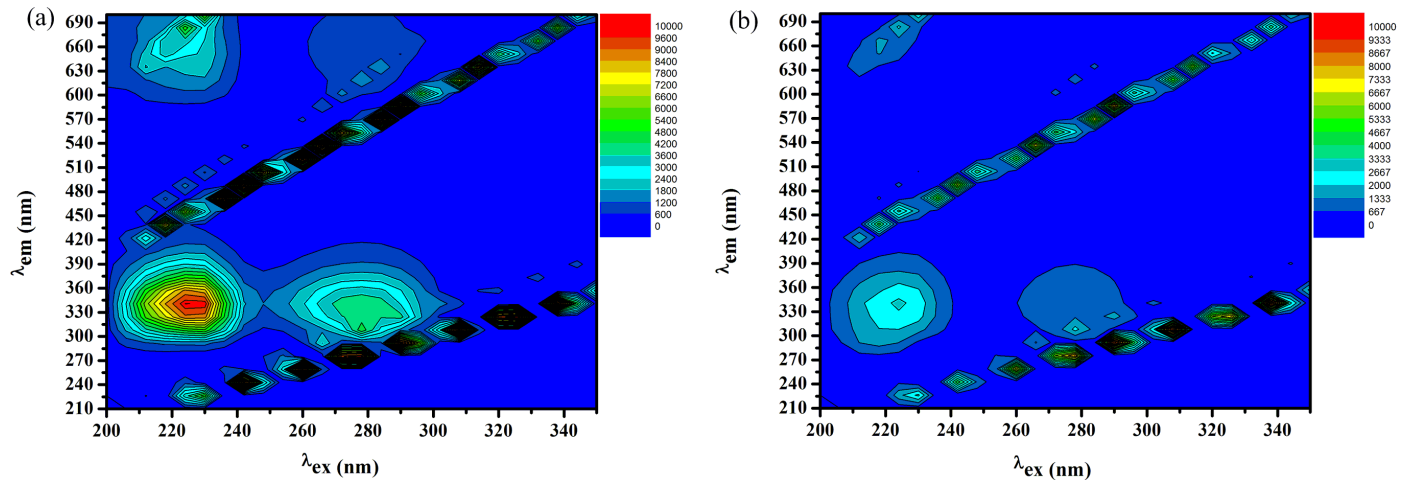


Fig 8. Contour plot of the fluorescence intensity spectra of BSA (a) AFB-BSA system (b).

doi:10.1371/journal.pone.0146297.g008

Supporting Information

S1 Fig. Binding mode and binding sites. Plots of $\log[(F_0-F)/F]$ vs. $\log[C_Q]$ for AFB-BSA interaction at different temperatures.

(PDF)

Acknowledgments

The authors would like to extend their sincere appreciation to the Deanship of Scientific Research at King Saud University for its funding this Research Group No. RG-1435-025

Author Contributions

Conceived and designed the experiments: AMA ASA. Performed the experiments: ASA. Analyzed the data: AMA ASA. Contributed reagents/materials/analysis tools: AMA. Wrote the paper: AMA ASA.

References

1. Stopfer P, Marzin K, Narjes H, Gansser D, Shahidi M, Uttereuther-Fischer M, et al. (2012) Afatinib pharmacokinetics and metabolism after oral administration to healthy male volunteers. *Cancer Chemother Pharmacol* 69: 1051–1061. doi: [10.1007/s00280-011-1803-9](https://doi.org/10.1007/s00280-011-1803-9) PMID: [22200729](https://pubmed.ncbi.nlm.nih.gov/22200729/)
2. U.S. Food and Drug Administration (FDA) (12th July 2013) Afatinib. In: Center for drug evaluation and Research, editor. MD, USA.
3. Kragh-Hansen U (1981) Molecular aspects of ligand binding to serum albumin. *Pharmacol Rev* 33: 17–53. PMID: [7027277](https://pubmed.ncbi.nlm.nih.gov/7027277/)
4. He XM, Carter DC (1992) Atomic structure and chemistry of human serum albumin. *Nature* 358: 209–215. PMID: [1630489](https://pubmed.ncbi.nlm.nih.gov/1630489/)
5. Bhattacharya AA, Grune T, S C (2000) Crystallographic analysis reveals modes of binding of medium and long chain fatty acids to human serum albumin. *Journal of Molecular Biology* 303: 721–732. PMID: [11061971](https://pubmed.ncbi.nlm.nih.gov/11061971/)
6. Sattar Z, Iranfar H, Asoodeh A, Saberi MR, Mazhari M, Chamani J (2012) Interaction between holo transferrin and HSA–PPIX complex in the presence of lomefloxacin: An evaluation of PPIX aggregation in protein–protein interactions. *Spectrochimica Acta Part A: Molecular and Biomolecular Spectroscopy* 97: 1089–1100.

7. Spector AA, John K, Fletcher JE (1969) Binding of long-chain fatty acids to bovine serum albumin. *Journal of Lipid Research* 10: 56–67. PMID: [5773785](#)
8. Borissevitch IE, Tominaga TT, Imasato H, Tabak M (1996) Fluorescence and optical absorption study of interaction of two water soluble porphyrins with bovine serum albumin. The role of albumin and porphyrin aggregation. *Journal of Luminescence* 69: 65–76.
9. Blauer G, King TE (1970) Interactions of bilirubin with bovine serum albumin in aqueous solution. *Journal of Biological Chemistry* 245: 372–381. PMID: [5460890](#)
10. Tian J, Liu J, Hu Z, Chen X (2005) Interaction of wogonin with bovine serum albumin. *Bioorganic & Medicinal Chemistry* 13: 4124–4129.
11. Zhou N, Liang YZ, Wang P (2007) 18 β -Glycyrrhetic acid interaction with bovine serum albumin. *Journal of Photochemistry and Photobiology A: Chemistry* 185: 271–276.
12. Wang YQ, Zhang HM, Zhang GC, Tao WH, Fei ZH, Liu ZT (2007) Spectroscopic studies on the interaction between silicotungstic acid and bovine serum albumin. *Journal of Pharmaceutical and Biomedical Analysis* 43: 1869–1875. PMID: [17280811](#)
13. Wang YP, Wei YL, Dong C (2006) Study on the interaction of 3,3-bis(4-hydroxy-1-naphthyl)-phthalide with bovine serum albumin by fluorescence spectroscopy. *Journal of Photochemistry and Photobiology A: Chemistry* 177: 6–11.
14. Bolel P, Mahapatra N, Halder M (2012) Optical Spectroscopic Exploration of Binding of Cochineal Red A with Two Homologous Serum Albumins. *Journal of Agricultural and Food Chemistry* 60: 3727–3734. doi: [10.1021/jf205219w](#) PMID: [22397587](#)
15. Carter DC, Ho JX (1994) Structure of Serum Albumin. *Advances in Protein Chemistry* 45: 153–203. PMID: [8154369](#)
16. Gong A, Zhu X, Hu Y, Yu S (2007) A fluorescence spectroscopic study of the interaction between epristeride and bovin serum albumine and its analytical application. *Talanta* 73: 668–673. doi: [10.1016/j.talanta.2007.04.041](#) PMID: [19073087](#)
17. Zhou B, Qi Z-D, Xiao Q, Dong J-X, Zhang Y-Z, Liu Y (2007) Interaction of loratadine with serum albumins studied by fluorescence quenching method. *Journal of biochemical and biophysical methods* 70: 743–747. PMID: [17482267](#)
18. Sułkowska A (2002) Interaction of drugs with bovine and human serum albumin. *Journal of Molecular Structure* 614: 227–232.
19. Shen G-F, Liu T-T, Wang Q, Jiang M, Shi J-H (2015) Spectroscopic and molecular docking studies of binding interaction of gefitinib, lapatinib and sunitinib with bovine serum albumin (BSA). *Journal of Photochemistry and Photobiology B: Biology* 153: 380–390.
20. Shi J-H, Chen J, Wang J, Zhu Y-Y, Wang Q (2015) Binding interaction of sorafenib with bovine serum albumin: Spectroscopic methodologies and molecular docking. *Spectrochimica Acta Part A: Molecular and Biomolecular Spectroscopy* 149: 630–637.
21. Sugio S, Kashima A, Mochizuki S, Noda M, Kobayashi K (1999) Crystal structure of human serum albumin at 2.5 Å resolution. *Protein Engineering* 12: 439–446. PMID: [10388840](#)
22. Petitpas I, Grüne T, Bhattacharya A, Curry S (2001) Crystal structures of human serum albumin complexed with monounsaturated and polyunsaturated fatty acids. *Journal of Molecular Biology* 314: 955–960. PMID: [11743713](#)
23. Zhang H-x, Gao S, Yang X-x (2009) Synthesis of an octupolar compound and its biological effectson serum albumin. *Molecular Biology Reports* 36: 1405–1411. doi: [10.1007/s11033-008-9329-x](#) PMID: [18704755](#)
24. Dufour C, Dangles O (2005) Flavonoid–serum albumin complexation: determination of binding constants and binding sites by fluorescence spectroscopy. *Biochimica et Biophysica Acta (BBA)-General Subjects* 1721: 164–173.
25. Lakowicz JR (2007) *Principles of fluorescence spectroscopy*: Springer Science & Business Media.
26. Pasban Ziyarat F, Asoodeh A, Sharif Barfeh Z, Pirouzi M, Chamani J (2014) Probing the interaction of lysozyme with ciprofloxacin in the presence of different-sized Ag nano-particles by multispectroscopic techniques and isothermal titration calorimetry. *Journal of Biomolecular Structure and Dynamics* 32: 613–629. doi: [10.1080/07391102.2013.785919](#) PMID: [23659247](#)
27. Bourassa P, Bariyanga J, Tajmir-Riahi HA (2013) Binding Sites of Resveratrol, Genistein, and Curcumin with Milk α - and β -Caseins. *The Journal of Physical Chemistry B* 117: 1287–1295. doi: [10.1021/jp3114557](#) PMID: [23305484](#)
28. Hu Y, Da L (2014) Insights into the selective binding and toxic mechanism of microcystin to catalase. *Spectrochimica Acta Part A: Molecular and Biomolecular Spectroscopy* 121: 230–237.
29. Lakowicz JR (1999) *Principle of fluorescence spectroscopy*. New York: Plemum Press.

30. Wang H, Mao J, Duan A, Che B, Wang W, Ma M, et al. (2013) Fluorescence Quenching of 4-tert-Octylphenol by Room Temperature Ionic Liquids and its Application. *J Fluoresc* 23: 323–331. doi: [10.1007/s10895-012-1150-1](https://doi.org/10.1007/s10895-012-1150-1) PMID: [23207872](https://pubmed.ncbi.nlm.nih.gov/23207872/)
31. Chen G-Z, Huang X-Z, Xu J-G (1990) *Spectrofluorimetric Analytical Method*. Beijing: Science Press.
32. Shcharbin D, Klajnert B, Mazhul V, Bryszewska M (2005) Dendrimer Interactions with Hydrophobic Fluorescent Probes and Human Serum Albumin. *J Fluoresc* 15: 21–28. PMID: [15711873](https://pubmed.ncbi.nlm.nih.gov/15711873/)
33. Stern O, Volmer M (1919) The extinction period of fluorescence. *Phys Z* 20: 183–188.
34. Lineweaver H, Burk D (1934) The Determination of Enzyme Dissociation Constants. *Journal of the American Chemical Society* 56: 658–666.
35. Ware WR (1962) Oxygen Quenching Of Fluorescence In Solution: An Experimental Study Of The Diffusion Process. *The Journal of Physical Chemistry* 66: 455–458.
36. Huang Y, Zhang Z, Zhang D, Lv J (2001) Flow-injection analysis chemiluminescence detection combined with microdialysis sampling for studying protein binding of drug. *Talanta* 53: 835–841. PMID: [18968173](https://pubmed.ncbi.nlm.nih.gov/18968173/)
37. Lakowicz JR, Weber G (1973) Quenching of fluorescence by oxygen. Probe for structural fluctuations in macromolecules. *Biochemistry* 12: 4161–4170. PMID: [4795686](https://pubmed.ncbi.nlm.nih.gov/4795686/)
38. Liu J, Tian J-n, Zhang J, Hu Z, Chen X (2003) Interaction of magnolol with bovine serum albumin: a fluorescence-quenching study. *Analytical and Bioanalytical Chemistry* 376: 864–867. PMID: [12830359](https://pubmed.ncbi.nlm.nih.gov/12830359/)
39. Forster T, Sinanoglu O (1996) *Modern Quantum Chemistry*. New York: Academic Press. 93 p.
40. Abdelhameed AS (2015) Insight into the Interaction between the HIV-1 Integrase Inhibitor Elvitegravir and Bovine Serum Albumin: A Spectroscopic Study. *Journal of Spectroscopy* 2015.
41. Abdelhameed AS, Alanazi AM, Kadi AA (2015) Spectrofluorimetric study of finasteride and bovine serum albumin interaction and its application for quantitative determination of finasteride in tablet dosage form. *Analytical Methods*.
42. Rub MA, Khan JM, Asiri AM, Khan RH, ud-Din K (2014) Study on the interaction between amphiphilic drug and bovine serum albumin: A thermodynamic and spectroscopic description. *Journal of Luminescence* 155: 39–46.
43. Ross PD, Subramanian S (1981) Thermodynamics of protein association reactions: forces contributing to stability. *Biochemistry* 20: 3096–3102. PMID: [7248271](https://pubmed.ncbi.nlm.nih.gov/7248271/)
44. Liu J, Tian J, He W, Xie J, Hu Z, Chen X (2004) Spectrofluorimetric study of the binding of daphnetin to bovine serum albumin. *Journal of Pharmaceutical and Biomedical Analysis* 35: 671–677. PMID: [15137995](https://pubmed.ncbi.nlm.nih.gov/15137995/)
45. Yan H, Zhao S, Yang J, Zhu X, Dai G, Liang H, et al. (2009) Interaction Between Levamisole Hydrochloride and Bovine Serum Albumin and the Influence of Alcohol: Spectra. *Journal of Solution Chemistry* 38: 1183–1192.
46. Zhang H-X, Huang X, Mei P, Gao S (2008) Interaction between Glyoxal-bis-(2-hydroxyanil) and Bovine Serum Albumin in Solution. *Journal of Solution Chemistry* 37: 631–640.
47. Glazer AN, Smith EL (1961) Studies on the Ultraviolet Difference Spectra of Proteins and Polypeptides. *Journal of Biological Chemistry* 236: 2942–2947. PMID: [13899166](https://pubmed.ncbi.nlm.nih.gov/13899166/)